

# Generalized Anomaly Detection

Suresh Singh, Minwei Luo, Yu Li

Portland State University  
singh@cs.pdx.edu, minwei1L@outlook.com, liyu\_0705@outlook.com

## Abstract

We study anomaly detection for the case when the *normal* class consists of more than one object category. This is an obvious generalization of the standard one-class anomaly detection problem. However, we show that jointly using multiple one-class anomaly detectors to solve this problem yields poorer results as compared to training a single one-class anomaly detector on all normal object categories together. We further develop a new anomaly detector called DeepMAD that learns compact distinguishing features by exploiting the multiple normal objects categories. This algorithm achieves higher AUC values for different datasets compared to two top performing one-class algorithms that either are trained on each normal object category or jointly trained on all normal object categories combined. In addition to theoretical results we present empirical results using the CIFAR-10, fMNIST, CIFAR-100, and a new dataset we developed called RECYCLE.

## 1 Introduction

To motivate this formulation of anomaly detection, let us consider several applications: imagine a roadside garbage container that automatically separates any discarded trash into recycles (glass, cans, plastic, etc.) or garbage; machines used to separate normal blood cells (monocytes, neutrophils, basophils, etc.) from bacteria in the blood (sepsis); generic classification problems such as separating all species of cats from any other animal; separating sounds of different mosquito species from any other sound; and many, many more. In all these examples, the normal class in fact consists of several different object categories.

It is trivial to see that one-class anomaly detection algorithms (Ruff and et al. 2020b; Hendrycks, Mazeika, and Dietterich 2019; Goyal et al. 2020; Li et al. 2018; Lakhina, Crovella, and Diot 2004; Golan and El-Yaniv 2018; Ackay, Atapour-Abarghouei, and Breckopn 2018; Nguyen et al. 2019; Schlegl et al. 2017; Song et al. 2017; Ruff and et al. 2018; Nash et al. 1994) can be easily applied to this problem. In a typical one-class formulation, the classifier is only trained on in-distribution samples and it learns a probability density function  $P$  that captures normal behavior. Points that then map to a low probability region are classified as anomalous. Generalizing to the case when

$m$  different object categories are all considered normal, we can train  $m$  separate one-class anomaly detectors  $P_1, \dots, P_m$  and use them together to classify any new object. However, we show that this approach is not as good as training a single one-class anomaly detector on all the  $m$  categories combined. This result is demonstrated empirically as well as theoretically. The intuition is that errors in classification of each of the  $m$  one-class detectors are cumulative thus resulting in poor joint performance.

Novelty detection (Pimentel et al. 2014; Masana et al. 2018; Tack et al. 2020) and out-of-distribution (OOD) detection (Hendrycks and Gimpel 2017; Ren and et al 2019; Lakshminarayanan, Pritzel, and Blundell 2017; Lee et al. 2018a; Liang, Li, and Srikant 2018; Vyas et al. 2018) are related to anomaly detection but our model has significant differences. A common model used in OOD is to consider, for example, the fMNIST data set as normal and MNIST as OOD or CIFAR-10 as normal and natural images as OOD, etc. This model for defining what constitutes OOD has recently come under criticism (Ahmed and Courville 2020; Ren and et al 2019). As (Ahmed and Courville 2020) notes, *different datasets are created and curated differently* and thus it is likely that OOD algorithms are learning to identify these idiosyncrasies rather than meaningful features. Similarly, they argue that the context of the OOD task also matters – what is OOD in one context may not be OOD in another. (Ren and et al 2019) also argues for more realistic benchmarks for OOD (they use a bacteria genome database) observing that distributional shifts learned in traditional OOD tasks may have learned the background and thus have high error when used for realistic tasks. Finally, (Ahmed and Courville 2020) proposes testing OOD algorithms by sticking to the same dataset. They study the case when 9 out of 10 CIFAR-10 classes are normal and the tenth is treated as anomalous. We note that our model follows this approach. We study cases when 2, 5, 9 classes of CIFAR-10, MNIST, and fMNIST are normal while the others are anomalous.

In novelty detection, a data point is considered an outlier if it differs significantly from a collection of normal data points (e.g., a mammogram with a lump is an outlier in a collection of normal mammograms). The outlier and the normal data points can be seen as being similar and what distinguishes the outlier is its distance from a majority of normal

points. A multi-class novelty model is an extension where the number of outliers is large enough to form a separate cluster but all the points are still similar. *In our multi-class model, on the other hand, the normal classes can be arbitrary* (e.g., the normal classes may be dog and truck images).

There are two variations of the multi-class anomaly detection problem – the class labels of normal samples may either be unknown or known during training. We call these two formulations *inseparable* and *separable* respectively and we study both in this paper. The major results of our paper can be summarized as follows:

- We prove that training a one-class classifier in the inseparable case yields a higher AUC (Area Under the Curve) value than training multiple single-class classifiers for the separable case and combining their outputs. Our proof uses the formulation for combining probabilities from the theory of *belief functions*, Lemma 3.1.
- We illustrate these results using two recent one-class anomaly detection algorithms DROCC (Goyal et al. 2020) and DeepSVDD (Ruff and et al. 2020a) for the task of multi-class anomaly detection. We did not use OOD algorithms such as (Hendrycks and Gimpel 2017) because, as noted previously (Ahmed and Courville 2020), these algorithms train on one dataset and test on another and likely learn dataset idiosyncrasies rather than meaningful image features.
- We present a new algorithm called DeepMAD for the *separable case* and compare the accuracy of DeepMAD and two versions of each of DROCC and DeepSVDD (in one version we train  $m$  separate one-class classifiers and in the other we train a single one-class classifier by combining training data from all  $m$  normal classes). These five algorithms are compared using CIFAR-10, fMNIST, CIFAR-100, and RECYCLE. The RECYCLE dataset is one we created to study the problem of classifying recycles described in the first paragraph of this section. We show that DeepMAD performs well above all other algorithms by a wide margin.

## 2 Related Work

A variety of one-class novelty detection algorithms exist (Zhang et al. 2020; Masana et al. 2018; Chen et al. 2020; Tax and Duin 2004; Hoffmann 2007; Sabokrou et al. 2018; Pidhorskyi et al. 2018; Abati et al. 2019) but, as noted previously (Perera, Nallapati, and Xiang 2019), these algorithms are not directly applicable to the single-class anomaly detection problem. In the latter case we assign labels whereas in the former we learn a latent space that separates the normal class effectively from outliers. There have been a few additional works that consider a multi-class novelty detection problem (Perera and Patel 2019) where the dataset is split into two subsets of classes with one treated as normal. A large reference labeled dataset is used in conjunction with normal samples during training. Our problem formulation differs from this in that we do not use any reference dataset as a comparator to extract features. We also consider cases when the split of normal/anomaly classes is variable.

In OOD detection, out of distribution samples are detected via the basic predictive confidence of the classifier (MSP score) (Hendrycks and Gimpel 2017) or measures such as temperature-scaled softmax scores (ODIN) (Liang, Li, and Srikant 2018) or confidence calibration (DeVries and Taylor 2018). Approaches as in (Hendrycks, Mazeika, and Dietterich 2019) use other datasets as proxies for OOD examples while (Lee et al. 2018a) uses a GAN to generate negative examples for training. Other methods to improve the representation of in-distribution data includes using self-supervised approaches such as contrastive learning (Chen et al. 2020), alternative training strategies such as margin loss (Vyas et al. 2018), or metric learning (Masana et al. 2018). (Bergman and Hoshen 2020) splits normal data into  $M$  and learns features to separate them.

Early approaches to one-class anomaly detection relied on mostly hand-constructed features (Lakhina, Crovella, and Diot 2004). Other early methods such as one-class SVM (Tax and Duin 2004), density estimation (Vandermeulen and Scott 2013), and others (Liu, Ting, and Zhou 2008) are limited in their scalability. More recently, *deep learning* based methods have been used to address this problem. For instance (Ruff and et al. 2020a, 2018) describes DeepSVDD in which a deep neural network is trained to map the in-class data into a sphere of minimal volume, while (Ghafoori and Leckie 2020) maps to multiple spheres. DROCC (Goyal et al. 2020) trains the network to distinguish manufactured out of distribution points that are perturbations of in-distribution points as a way to learn more discriminating features. Another approach has been to train auto encoders to learn a lower dimensional representation (Li et al. 2018; Nguyen et al. 2019; Schlegl et al. 2017). An entirely different way of looking at the problem is to use self-supervision by learning *transformations* where a new sample is classified as normal if transforms applied to it can be correctly identified (Golan and El-Yaniv 2018; Hendrycks et al. 2019; Sohn et al. 2021).

## 3 Generalizing Single-Class Anomaly Detection to the Multi-Class Case

Typically, anomaly detection methods learn a mapping  $\mathcal{F}$  from the input space  $\mathcal{X}$  to some lower dimensional feature space  $\mathcal{Y}$ . Inputs are then assigned a probability of being normal or anomalous via some function  $D$ .  $\mathcal{F}$  is learned using the normal class examples while  $D$  may be static (e.g., a distance measure of points in feature space) or jointly learned. If we consider using one-class anomaly detectors for the multi-class case where there are  $1 \leq i \leq m$  normal classes, for each class we learn one classifier giving us a set  $\{(\mathcal{F}_i, D_i)\}_{i=1}^m$  of one-class anomaly detectors. The question then is how to use these  $m$  detectors for the multi-class case.

We can use the theory of *belief functions* in risk analysis (Clemen and Winkler 1999) to provide a framework for combining these  $m$  classifiers. In this theory, the assumption is that  $m$  experts provide their own assessment of risk among a set of choices. In order to develop a final estimate of risk, these  $m$  estimates are combined. In the stan-

	$\{1\}$	$\{2\}$	$\dots$	$\{m\}$	$\neg\{1\}$	$\neg\{2\}$	$\dots$	$\neg\{m\}$
$(\mathcal{F}_1, D_1)$	$P_1(1 x)$	0	$\dots$	0	$1 - P_1(1 x)$	0	$\dots$	0
$\vdots$	$\vdots$	$\vdots$	$\dots$	$\vdots$	$\vdots$	$\vdots$	$\dots$	$\vdots$
$(\mathcal{F}_m, D_m)$	0	0	$\dots$	$P_m(m x)$	0	0	$\dots$	$1 - P_m(m x)$

Table 1: Probability estimates for sample  $x \in \mathcal{X}$  provided by  $m$  classifiers.

standard formulation of the problem, as applied to our case, let  $U = \{1, 2, \dots, m, \Lambda\}$  denote the set of  $m$  normal classes (1 to  $m$ ) and a catchall class labeled  $\Lambda$  which represents all *anomalies*. A general classifier assigns a probability  $P(u|x)$  for the probability that an image  $x$  belongs to the *set of classes*  $u$ , where  $u \in 2^U$  is an element of the powerset of  $U$ . For example if  $u = \{1, 5\}$  then this is the probability that  $x$  belongs to either of the classes 1 or 5.

This general formulation simplifies considerably for our case because the one-class classifiers will only assign a non-zero probability to two instances, as illustrated in Table 2. In other words,  $P_i(u|x) = 0$  for all cases except when  $u = \{i\}$  or  $u = \neg\{i\} = \{1, 2, \dots, i-1, i+1, \dots, m, \Lambda\}$ . In order to combine the predictions of the  $m$  one-class classifiers to compute the probability that  $x$  is anomalous, we need to determine  $P(\Lambda|x)$ . According to the Dempster-Schafer Theory (Dempster 1967; Shafer 1976) (please see Appendix A for a simple example),

$$P(\Lambda|x) = \frac{1}{K} \sum_{\neg\{1\} \cap \neg\{2\} \cap \dots \cap \neg\{m\} = \Lambda} \prod_{i=1}^m P_i(\neg\{i\}|x) \quad (1)$$

which simplifies to,

$$P(\Lambda|x) = \frac{1}{K} \prod_{i=1}^m P_i(\neg\{i\}|x) \quad (2)$$

since there is just one case when the intersection of the predictions of the  $m$  classifiers yields  $\Lambda$ .  $K$  is given by,

$$K = 1 - \sum_{u_1 \cap u_2 \cap \dots \cap u_m = \phi} \prod_{i=1}^m P_i(u_i|x) \quad (3)$$

where  $u_i \in \{\{i\}, \neg\{i\}\}$  (because all other probabilities are zero from Table 1, these are the only non-trivial cases). The above equation simplifies to,

$$K = \prod_{i=1}^m P_i(\neg\{i\}|x) + \sum_{i=1}^m P_i(\{i\}|x) \prod_{j=1, j \neq i}^m P_j(\neg\{j\}|x) \quad (4)$$

From the above formulation it follows that an input  $x$  is classified as normal if *any* of the  $m$  classifiers say it is normal and it is classified as anomalous if *all* classifiers classify it as anomalous. Thus, it is easy to construct a multi-class anomaly detection algorithm using  $m$  one-class anomaly detectors as shown in Algorithm 1.

Another approach for training a one-class classifier for the  $m$  class case is to simply combine the training data from all  $m$  classes and treat that as a single class. Doing so gives us Algorithm 2 below. We state the following results (proofs are in Appendix B) about the two algorithms.

---

#### Algorithm 1: Using $m$ Single-Class Anomaly Detection for Multi-Class Case.

---

*Training:* Let  $(\mathcal{F}, D)$  be any one-class anomaly detection algorithm. Given training set  $X = \{X_1, X_2, \dots, X_m\}$  consisting of training examples from  $m$  classes  $X_i \subset \mathcal{X}_i$ , train  $(\mathcal{F}, D)$  separately on each class producing  $m$  classifiers,  $(\mathcal{F}_i, D_i) 1 \leq i \leq m$ .

*Testing:* Given  $x \in \mathcal{X}$ , classify it with each of the  $m$  classifiers. *Declare  $x$  anomalous if all classifiers classify it as anomalous.*

*Notes:* A classifier  $(\mathcal{F}, D)$  typically uses a comparison  $D(\mathcal{F}(x)) < T$  for classification ( $T$  is an arbitrary threshold that can be tuned). For SVDD this is a distance from the center while for DROCC it is distance from a manifold.

---

**Lemma 3.1** *Algorithm 2 has a higher AUC value than Algorithm 1 when the same one-class anomaly detection algorithm is used in both cases.*

**Corollary 3.1.1** *As  $m$  increases, the AUC value for Algorithm 1 decreases.*

Note that this corollary is not true for Algorithm 2.

---

#### Algorithm 2: Training a *single* classifier by combining all $m$ classes.

---

*Training:* Given a training set  $X = X_1 \cup X_2 \cup \dots \cup X_m$ , train a single classifier  $(\mathcal{F}, D)$  on this set (see *Notes* in Algorithm 1).

*Testing:* An example  $x$  is classified as normal or anomalous by this classifier (just like any single-class classifier).

*Notes:* This algorithm can be applied directly to the *inseparable* model described previously.

---

### 3.1 Algorithms Studied

In this paper, we use two recent and high performing single-class anomaly detection algorithms – DROCC (Goyal et al. 2020) and DeepSVDD (Ruff and et al. 2020a). For each algorithm we consider two variations corresponding to Algorithms 1 & 2 above. Thus, DROCC( $m$ ) and DeepSVDD( $m$ ) correspond to Algorithm 1 while DROCC and DeepSVDD correspond to Algorithm 2. We use the author provided code for our experiments.

## 4 DeepMAD: Deep Multi-class Anomaly Detection

Our algorithm DeepMAD is based on Algorithm 1 above, but with important changes. The key insights we applied are the following:

- For any single-class algorithm, AUC values increase if the *variance* of the pdf of the normal class is reduced because it increases the TPR (True Positive Rate) without affecting the FPR (False Positive Rate), assuming the means of the normal and anomaly classes do not shift.
- In the absence of anomalies, the features learned represent what is *common* among the examples. DROCC attempts to learn *discriminating* features by using the manufactured examples. Similarly, algorithms that add noise to training examples or that learn transformations etc. are all attempting to reduce variance by learning discriminating features..
- When moving to the multi-class case, observe that Algorithm 2 will likely learn features common among the normal classes in addition to features common to examples within each class, potentially resulting in larger variance.

In DeepMAD, we train  $m$  one-class anomaly detectors. However, rather than train  $P_i$  only on the  $i$ th normal class, we train it on all  $m$  classes where we use the training examples from classes  $\neg\{i\}$  as anomalous.

---

#### Algorithm 3: DeepMAD

---

*Training:* Randomly initialize  $m$  autoencoders  $A_i$ ;  
 For every  $A_i$ , train  $A_i$  on provided examples  $X_i$ ;  
 Using the encoder part  $E_i$  of the autoencoder, identify a point  $c_i$ , the "center" for this class;  
 For every encoder  $E_i$ , create *labeled* training data  $\{(x, l) \mid x \in X_i \text{ then } l = +1 \text{ else if } x \in \bigcup_{j=1, j \neq i}^m X_j \text{ then } l = -1\}$ .  
 Then train  $E_i$  on this data using loss function  $\mathcal{L}$   
*Result:*  $m$  trained encoders  $E_i$

*Testing:* Given  $x$  to classify,  
 Compute  $d(x) = \min_{i=1}^m \|c_i - E_i(x; \theta_i)\|_2$ ;  
 If  $d(x) < \gamma$  then  $x$  is *normal* else  $x$  is *anomalous*

---

The algorithm for training proceeds in two steps. For every class  $i$ , we first train an autoencoder  $A_i$  using MSE between the original and reconstructed image as the loss. Next, we train only the encoder  $E_i$  using the other  $m - 1$  classes as anomalies and class  $i$  as normal. For this, we identify a "center"  $c_i$  for this class and learn a representation that maps points in  $X_i$  to a sphere around it and maps other points from the remaining classes far away. We use the following loss function,

$$\mathcal{L}(\theta_i) = \frac{1}{N} \sum_{j=1}^{N_i} \|E_i(x_j; \theta_i) - c_i\|^2 + \frac{\eta}{N} \sum_{x_k \in (\bigcup_j X_j) \setminus X_i} (\max(0, \delta - \|E_i(x_k; \theta_i) - c_i\|_2)^2) + \frac{\lambda}{2} \sum_{l=1}^L \|W^l\|_F^2$$

where  $N = |X_1| + \dots + |X_m|$  is the total number of normal class samples and  $N_i = |X_i|$  is the number of examples from normal class  $i$ .  $\delta, \eta$  and  $\lambda$  are hyperparameters where  $\eta$  controls the weight given to the *contrastive loss* term,  $\delta$  is a distance from the identified center beyond which we would like to map points not in  $X_i$ , and  $\lambda$  is a regularization parameter. The first term above attempts to learn a small sphere about the center for normal points in class  $i$  while the second term attempts to maximize the distance of the remaining

normal points (all except points in  $X_i$ ) far away. The ensemble method in (Vyas et al. 2018) also trains multiple classifiers and uses a mean of their softmax outputs for OOD detection. Unlike our work, they train on one dataset and test on another (recall the criticism from (Ahmed and Courville 2020) which notes that detecting anomalies within the same dataset is much harder than between datasets). It is also unclear how well their method would scale down to few normal classes (say 2).

## 5 Empirical Evaluation

We compare the performance of five algorithms – DROCC, DROCC( $m$ ), DeepSVDD, DeepSVDD( $m$ ), and DeepMAD using four data sets: CIFAR-10, fMNIST, RECYCLE, and CIFAR-100. For DROCC and DeepSVDD we used the code provided by the authors while for the  $m$  normal classes case we simply replicated the code and modified the main() function appropriately. For all the experiments with DROCC, we used parameters radius  $r = 8$ ,  $\mu = 1$ , learning rate = 0.001, ascent step = 0.001 and the Adam optimizer. The reason for this choice is that the ablation study reported in (Goyal et al. 2020) shows a fairly stable AUC value for this parameter setting across classes (though the specific value for  $r$  that achieves optimal AUC for the single-class case can vary by class). The parameter settings for DeepSVDD used  $\eta = 1$ , learning rate of 0.0001 and the Adam optimizer as well. We consider three multi-class anomaly detection cases for CIFAR-10 and fMNIST – (2/8), (5/5), and (9/1) which correspond to 2, 5, 9 normal classes respectively. For CIFAR-100 we used the 20 super-classes and studied the (2/18) case. For the RECYCLE dataset (described below) we have 5 classes of recyclables and one that is assorted trash. We considered two cases: in one, we study the (4/1) case using only the recycles; we then study the case when the 5 recycles are all normal and the trash is the anomaly. In all cases we repeated the experiments with random seeds and report the 95% confidence intervals of the achieved AUC values.

The RECYCLE dataset contains 5 classes of recycles – glass bottles, plastic bottles, cans, crushed cans, and cardboard boxes. The original images were 3008x2000x3 but we downsampled them to 32x32x3. There are a total of 11,000 images evenly divided among the five classes. 10,000 are used for training and 1,000 for testing. Samples of these images are shown in Figure 1. We also created 300 *trash* images to use for testing. Some examples are shown in Figure 2.

Table 2 summarizes the AUC values achieved by each of the five algorithms on CIFAR-10. For the (2/8) case, there are 45 combinations, for (5/5) there are 252 and for (9/1) there are ten. In the table we report on the range of values with their confidence intervals. For all three cases we note that DeepMAD has the best AUC values (with the exception of an outlier for DROCC). But more importantly, observe that DROCC performs better than DROCC( $m$ ) and DeepSVDD performs better than DeepSVDD( $m$ ), which is what the theoretical results from the previous section predicted. Figure 3 provides a scatter plot of all 45 combinations for the five algorithms for the case when two classes

	2-in, 8-out	5-in, 5-out	9-in, 1-out
DROCC	0.4728 $\longleftrightarrow$ 0.7252 $\pm 0.0119$ $\pm 0.0081$	0.4316 $\longleftrightarrow$ 0.7219 $\pm 0.0257$ $\pm 0.0039$	0.4107 $\longleftrightarrow$ 0.7146 $\pm 0.0454$ $\pm 0.0079$
Outlier	(0, 8) 0.8359 $\pm 0.0117$		
DROCC( $m$ )	0.4216 $\longleftrightarrow$ 0.6912 $\pm 0.0424$ $\pm 0.0188$	0.3806 $\longleftrightarrow$ 0.7023 $\pm 0.0047$ $\pm 0.0648$	0.3439 $\longleftrightarrow$ 0.6896 $\pm 0.1034$ $\pm 0.0453$
Outlier	(0, 8) 0.8255 $\pm 0.0137$		
DeepSVDD	0.4088 $\longleftrightarrow$ 0.7623 $\pm 0.0068$ $\pm 0.0193$	0.3382 $\longleftrightarrow$ 0.7105 $\pm 0.0076$ $\pm 0.0077$	0.3058 $\longleftrightarrow$ 0.6844 $\pm 0.0169$ $\pm 0.0144$
DeepSVDD( $m$ )	0.4147 $\longleftrightarrow$ 0.7516 $\pm 0.0129$ $\pm 0.0093$	0.3482 $\longleftrightarrow$ 0.6909 $\pm 0.0123$ $\pm 0.0133$	0.3580 $\longleftrightarrow$ 0.5864 $\pm 0.0166$ $\pm 0.0167$
DeepMAD	0.5396 $\longleftrightarrow$ 0.7647 $\pm 0.0031$ $\pm 0.0014$	0.4929 $\longleftrightarrow$ 0.7738 $\pm 0.0046$ $\pm 0.0022$	0.5437 $\longleftrightarrow$ 0.7230 $\pm 0.0028$ $\pm 0.0084$

Table 2: AUC range for CIFAR-10



Figure 1: Examples of objects from the five (5) recycle classes.

are normal. It is clear that which classes are considered normal has a huge impact on AUC values. For all but DeepMAD, some cases have an AUC value below 0.5 which is very poor. Its noteworthy that the case when classes 0 and 8 are normal DROCC has a very high AUC value (labeled an outlier in the table). Figure 4 plots the AUC values for the ten best and ten worst cases (out of 252) for when 5 classes are normal. The specific class combinations that have the best and worst values are different for the algorithms (details are in the supplementary materials). Aside from the fact that DeepMAD performs better, it also shows considerably low variance. This points to it learning very good discriminating features. Plots of AUC values for CIFAR-100 and 9/1 case are in the Appendix (as are additional tables and data).

We ran DROCC, DeepSVDD, and DepMAD on the fMNIST, RECYCLE, and CIFAR-100 datasets as well. We did not run DROCC( $m$ ) and DeepSVDD( $m$ ) because, as we have seen, training over all classes jointly performs better. Table 3 provides AUC values for CIFAR-100 where we see that DeepMAD has about 10% improvement over the other algorithms. In this case we considered the 20 super-classes and considered just a single case when 2 of the 20 classes are considered normal. The table also provides AUC values for fMNIST. Here the picture is more mixed. For the case when 2 classes are normal, all algorithms are very similar with DeepSVDD holding a 2% edge when averaged over 45 combinations. DeepMAD performs better on average for the other two cases. For the RECYCLE dataset, DeepMAD performs well above the other two algorithms. The (4/1) case is when we only consider the five recycle classes and use four of them as defining normal with the fifth being the anomaly. We also considered the case when the five recycle classes were all normal and *trash* was considered as the anomaly. This is the (5/1) case in the table. All algorithms perform considerably better because trash images are very different

from recycles. However, DeepMAD is about 8% better than the other two.

## 5.1 Analysis of the Feature Vectors

To better explain the *big difference in AUC values seen by a given algorithm for different composition of normal classes*, we examine the feature vectors produced by DROCC, DeepSVDD, and DeepMAD for the 2/8 case for CIFAR-10. Each of the algorithms maps input images to  $D$  dimensional feature vectors (128 for DeepSVDD and DeepMAD and 64 for DROCC) which are used to find the distance of the vector from a ‘center’ (in DeepSVDD and DeepMAD) or from a manifold (in DROCC). These distances are compared with a threshold to determine if the point is normal or anomalous.

We studied one best case and one worst case for each of the algorithms. For DROCC this corresponded to (0,8) and (5,9) respectively, for DeepSVDD the cases are (4,6) and (1,5), and for DeepMAD we look at (0,1) and (3,5). For this analysis, we trained the classifier on the selected pair of normal classes and then ran 100 random images from each of the 10 class from the test sets of CIFAR-10 and saved the feature vectors (from the last layer) as well as the distance metric (to a center for DeepSVDD and DeepMAD) or the logits (for DROCC). We plot the cumulative distribution function (CDF) of the distance metric and logits in Figures 5, 6, and 7. For DeepSVDD it is clear that in (4,6) case, the learned mapping does separate different classes well from the two normal classes. However, for the (1,5) case, there are three other classes whose CDF lies to the left of (1,5) meaning their points lie closer to the ‘center’. Clearly this will result in a large number of false positive cases. In the case of DROCC, for the (0,8) case, only class 6 lies to the left of (0,8) 80% of the time which will result in false positives, others lie to the right. For the (5,9) case, several classes lie to



Figure 2: Examples of trash (images are all random trash and cannot be divided into classes).

	fMNIST			RECYCLE		CIFAR-100
	2-in, 8-out	5-in, 5-out	9-in, 1-out	4-in, 1-out	5-in, 1-out	2-in, 18-out
DROCC	0.6873 $\leftrightarrow$ 0.9774 $\pm 0.0937 \pm 0.0049$	0.5738 $\leftrightarrow$ 0.9260 $\pm 0.0397 \pm 0.0307$	0.5408 $\leftrightarrow$ 0.8247 $\pm 0.0961 \pm 0.0507$	0.4447 $\leftrightarrow$ 0.7997 $\pm 0.0176 \pm 0.0719$	90.56	0.3548 $\leftrightarrow$ 0.7329 $\pm 0.0006 \pm 0.0971$
Mean	0.8161	0.7448	0.6992	0.6128		0.5638
Deep	0.6622 $\leftrightarrow$ 0.9871 $\pm 0.0502 \pm 0.0033$	0.5438 $\leftrightarrow$ 0.9279 $\pm 0.0274 \pm 0.0325$	0.4551 $\leftrightarrow$ 0.8825 $\pm 0.0285 \pm 0.0137$	0.3703 $\leftrightarrow$ 0.8728 $\pm 0.0207 \pm 0.0079$	90.12	0.4196 $\leftrightarrow$ 0.7185 $\pm 0.0077 \pm 0.0180$
SVDD						
Mean	<b>0.8538</b>	0.7269	0.6523	0.5791		0.5559
Deep	0.6434 $\leftrightarrow$ 0.9714 $\pm 0.0640 \pm 0.0011$	0.5732 $\leftrightarrow$ 0.8832 $\pm 0.0485 \pm 0.0137$	0.4860 $\leftrightarrow$ 0.9395 $\pm 0.0267 \pm 0.3466$	0.5906 $\leftrightarrow$ 0.8283 $\pm 0.0035 \pm 0.0073$	<b>98.38</b>	0.5384 $\leftrightarrow$ 0.8213 $\pm 0.0018 \pm 0.0012$
MAD						
Mean	0.8329	<b>0.7739</b>	<b>0.7613</b>	<b>0.6966</b>		<b>0.6580</b>

Table 3: AUC range for fMNIST, RECYCLE, and CIFAR-100

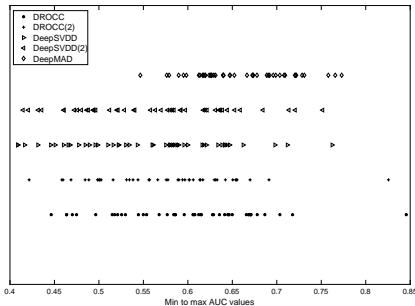


Figure 3: 2 in and 8 out case (CIFAR-10).

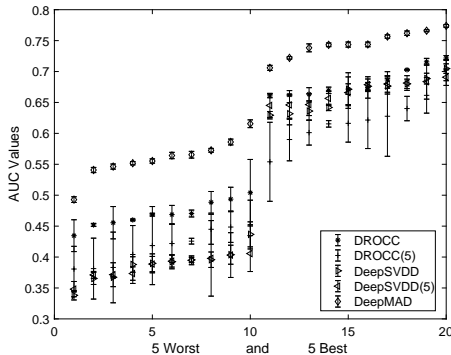


Figure 4: 5 in 5 out case (CIFAR-10).

the left of (5,9). A similar pattern is observed for DeepMAD as well.

While this analysis does give a partial explanation for the large range of AUC values, it does not give us much of an insight into why. We hypothesize that *feature vectors that are similar to one another will map similarly*. To apply this intuition, we need to contrast the empirical pdfs of all the feature vectors of all classes with respect to that of the normal classes. However, these are all multi-variate pdfs for which there is no accepted method available for comparison. Our approach is to employ the two sample *Kolmogorov-Smirnov* (KS) test to compare univariate distributions (we assume that the feature vectors elements are sampled from continuous distributions). The KS test considers the null hypothesis that the two provided set of points are from the same distribution. A value of 1 indicates that the null hypothesis is rejected at the given significance level (taken to be 5% here) meaning that the distributions are different. The KS test is typically used for one dimensional distributions only and thus apply the test to each dimension individually.

The method we apply is best explained using an example. Say DROCC is trained for in-distribution classes (0,8). We compute the KS statistic for every dimension for every class against the corresponding dimension of the pdf for (0,8). The values,  $\sum_{i=1}^D KS(\text{pdf class } (0,8) \text{ dim } i, \text{ pdf class } j \text{ dim } i)$  are computed for all classes  $j$ . Table 4 summarizes these values for all algorithms. For the DROCC maximum value can be 64 while for DeepSVDD DeepMAD the maximum value can be 128. We observe that DROCC has an almost optimal KS value for the case when (0,8) are the in-distribution classes (the best case with AUC of 0.84) whereas for (5,9) the average KS value is lower for class 1 implying that images from class 1 have a high likelihood of being incorrectly classified as normal. The values for DeepSVDD are smaller for the best and worst cases, though the worst case has half the average KS of the best case. Since DeepMAD learns two encoders (one for each normal

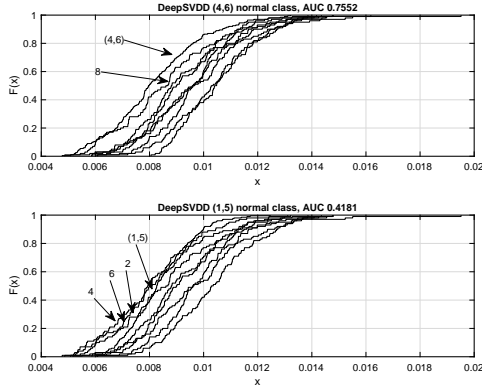


Figure 5: CDF of distances DeepSVDD.

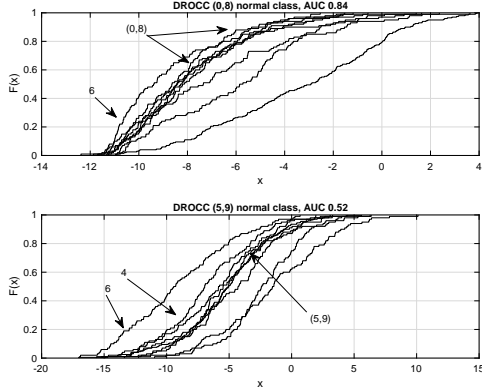


Figure 6: CDF of logits output by DROCC.

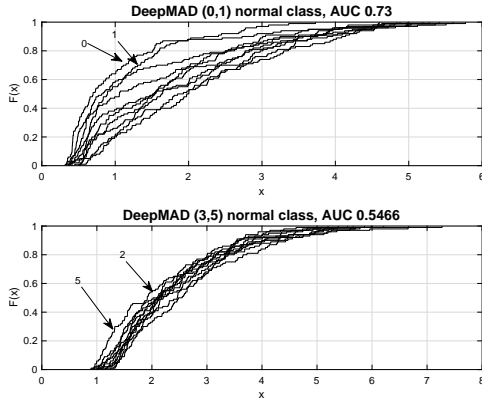


Figure 7: CDF of distances from ‘center’ DeepMAD.

DROCC									
0	1	2	3	4	5	6	7	8	9
KS((0,8),-), AUC = 0.84									
0	63	57	61	61	61	64	63	0	63
KS((5,9),-), AUC = 0.5									
45	12	36	50	51	14	52	31	38	14
DeepSVDD									
KS((4,6),-), AUC = 0.75									
37	45	9	30	0	24	0	29	36	49
KS((1,5),-), AUC = 0.41									
28	0	18	13	18	0	34	15	31	14
DeepMAD									
In classes (0,1), AUC=0.7174									
KS(0,-)									
0	100	44	127	124	128	126	128	60	125
KS(1,-)									
100	0	101	123	118	123	123	121	107	124
In classes (3,5), AUC=0.5277									
KS(3,-)									
6	1	4	0	16	96	2	73	81	99
KS(5,-)									
96	94	77	96	87	0	97	29	105	106

Table 4:  $h$  values for the KS test.

class) we report on the KS test values of each class against one of the normal classes. Again, we see a similar pattern with high KS values for the high AUC value case and low for the low AUC case.

## 6 Conclusions

The problem of multi-class anomaly detection occurs naturally in many settings, making it an important model to study. In this paper we adapt two one-class anomaly detection algorithms to the multi-class setting and develop a new algorithm DeepMAD. Our paper reports two significant results. First, we show that jointly learning a classifier (using single-class anomaly detection algorithms) for all the normal classes provides higher classification accuracy as compared to using several single-class classifiers. And second, we show that using supervised learning by treating  $m - 1$  out of  $m$  normal classes as anomalous results in much compact representations and hence uniformly higher accuracy. We compare our algorithm against two recent single-class classifiers adapted to the multi-class scenario and show improvements in AUC values for almost all cases for CIFAR-10, fMNIST, and and CIFAR-100. However, we still see AUC values below 0.7 for many cases and addressing this constitutes a major thrust of future work. We also take a first step in analyzing the feature vectors as a way to understand where the algorithms fail. We hope that the methodology we use for this analysis of feature vectors can be extended by others. Our code is available at <https://anonymous.4open.science/r/DeepMAD-33E1/README.md> and the RECYCLE dataset is available at <https://web.cecs.pdx.edu/~singh/rcyc-web/index.html>.



## References

- Abati, D.; Porrello, A.; Calderara, S.; and Cucchiara, R. 2019. AND: Autoregressive novelty detectors. In *Proceedings CVPR*.
- Ackay, A.; Atapour-Abarghouei, A.; and Breckopn, T. P. 2018. GANomaly: semi-supervised anomaly detection via adversarial training. In *Proceedings ACCV*, 622–637.
- Ahmed, F.; and Courville, A. 2020. Detecting Semantic Anomalies. In *Proceedings of AAAI*, volume 34, 3154–3162.
- Barnett, J. A. 1991. Calculating Dempster-Shafer Plausibility. *IEEE Transactions on Pattern Analysis and Machine Intelligence*, 13(6): 599–602.
- Bergman, L.; and Hoshen, Y. 2020. Classification-based anomaly detection for general data. In *Proceedings ICLR*.
- Caron, M.; Bojanowski, P.; Joulin, A.; and Douze, M. 2018. Deep clustering for unsupervised learning of visual features. In *Proceedings ECCV*, 132–149.
- Chen, T.; Kornblith, S.; Norouzi, M.; and Hinton, G. 2020. A simple framework for contrastive learning of visual representations. In *Proceedings ICML*.
- Choi, H.; Jang, E.; and Alemi, A. A. 2019. WAIC, but Why? Generative Ensembles for Robust Anomaly Detection. arXiv:1810.01392.
- Clemen, R. T.; and Winkler, R. L. 1999. Combining probability distributions from experts in risk analysis. *Risk Analysis*, 19(2): 187–203.
- Dempster, A. P. 1967. Upper and Lower Probabilities Induced by a Multivalued Mapping. *Annals of Mathematical Statistics*, 38(2): 325–339.
- DeVries, T.; and Taylor, G. W. 2018. Learning Confidence for Out-of-Distribution Detection in Neural Networks. arXiv:1802.04865.
- Ghafoori, Z.; and Leckie, C. 2020. Deep multi-sphere support vector data description. In *SIAM SDM*.
- Gidaris, S.; Singh, P.; and Komodakis, N. 2018. Unsupervised representation learning by predicting image rotations. In *Proceedings ICLR*.
- Golan, I.; and El-Yaniv, R. 2018. Deep anomaly detection using geometric transformations. In *Proceedings NeurIPS*.
- Gornitz, N.; Kloft, M.; Rieck, K.; and Brefeld, U. 2013. Toward supervised anomaly detection. *Journal of Artificial Intelligence Research*, 46: 235–262.
- Goyal, S.; Raghunathan, A.; M. Simhadri; and Jain, P. 2020. DROCC: Deep robust one-class classification. In *Proceedings ICML*.
- Hendrycks, D.; and Gimpel, K. 2017. A baseline for detecting misclassified and out-of-distribution examples in neural networks. In *Proceedings of ICLR*.
- Hendrycks, D.; Mazeika, M.; and Dietterich, T. 2019. Deep anomaly detection with outlier exposure. In *Proceedings ICLR*.
- Hendrycks, D.; Mazeika, M.; Kadavath, S.; and Song, D. 2019. Using self-supervised learning can improve model robustness and uncertainty. In *Proceedings NeurIPS*.
- Hoffmann, H. 2007. Kernel pca for novelty detection. *Pattern Recognition*, 40(3): 863–874.
- Lakhina, A.; Crovella, M.; and Diot, C. 2004. Diagnosing network wide traffic anomalies. *ACM SIGCOMM Computer Communications Review*, 34(4).
- Lakshminarayanan, B.; Pritzel, A.; and Blundell, C. 2017. Simple and scalable predictive uncertainty estimation using deep ensembles. In *31st Conference on Neural Information Processing Systems*.
- Lee, K.; Lee, H.; Lee, K.; and Shin, J. 2018a. Training Confidence-calibrated Classifiers for Detecting Out-of-Distribution Samples. arXiv:1711.09325.
- Lee, K.; Lee, K.; Lee, H.; and Shin, J. 2018b. A simple unified framework for detecting out-of-distribution samples and adversarial attacks. In *Proceedings NeurIPS*.
- Li, D.; Chen, D.; Goh, J.; and k. Ng, S. 2018. Anomaly detection with generative adversarial networks for multivariate time series. In *7th International Workshop on Big Data, Streams and Heterogeneous Source Mining: Algorithms, Systems, Programming Models and Applications (ACM KDD)*.
- Liang, S.; Li, Y.; and Srikant, R. 2018. Enhancing the reliability of out-of-distribution image detection in neural networks. In *Proceedings International Conference on Learned Representations (ICLR '18)*.
- Liu, F. T.; Ting, K. M.; and Zhou, Z.-H. 2008. Isolation forest. In *Proceedings ICDM*, 413–422.
- Masana, M.; Ruiz, I.; Serrat, J.; van de Weijer, J.; and Lopez, A. M. 2018. Metric learning for novelty and anomaly detection. In *British Machine Vision Conference*.
- Nash, W. J.; Sellers, T. L.; Talbot, S. R.; Cawthorn, A. J.; and Ford, W. B. 1994. The Population Biology of Abalone (Haliotis species) in Tasmania. I. Blacklip Abalone (*H. rubra*) from the North Coast and Islands of Bass Strait. Technical Report 48, Sea Fisheries Division, ISSN 1034-3288.
- Nguyen, D. T.; Lou, Z.; Klar, M.; and Brox, T. 2019. Anomaly detection with multiple-hypothesis predictions. In *Proceedings ICML*.
- Oza, P.; and Patel, V. M. 2019. One-class convolution neural network. *IEEE Signal Processing Letters*, 26(2): 277–281.
- Perera, P.; Nallapati, R.; and Xiang, B. 2019. OCGAN: one-class novelty detection using GANs with constrained latent representations. In *Proceedings CVPR*.
- Perera, P.; and Patel, V. M. 2019. Deep transfer learning for multiple class novelty detection. In *Proceedings CVPR*.
- Pidhorskyi, S.; Almohsen, R.; Adjeroh, D. A.; and Doretto, G. 2018. Generative probabilistic novelty detection with adversarial autoencoders. In *Proceedings NeurIPS*.
- Pimentel, M. A. F.; Clifton, D. A.; Clifton, L.; and Tarassenko, L. 2014. A review of novelty detection. *Signal Processing*, 215–249.
- Ren, J.; and et al. 2019. Likelihood ratios for out-of-distribution detection. In *33rd Conference on Neural Information Processing Systems*.



Ruff, L.; and et al. 2018. Deep One-Class Classification. In *Proceedings 35th International Conference on Machine Learning (ICML)*. Stockholm, Sweden.

Ruff, L.; and et al. 2020a. Deep Semi-Supervised Anomaly Detection. In *Proceedings ICLR*.

Ruff, L.; and et al. 2020b. A unifying review of deep and shallow anomaly detection. *arXiv:2009.11732v2*.

Sabokrou, M.; Khaloeei, M.; Fathy, M.; and Adeli, E. 2018. Adversarially learned one-class classifier for novelty detection. In *Proceedings CVPR*, 3379–3388.

Schlegl, T.; Seebock, P.; Waldstein, S. M.; Schmidt-Erfurth, U.; and Langs, G. 2017. Unsupervised anomaly detection with generative adversarial networks to guide marker discovery. In *International Conference on Information Processing in Medical Imaging*, 146–157.

Shafer, G. 1976. *Mathematical Theory of Evidence*. Princeton University Press.

Sohn, K.; Li, C.-L.; Yoon, J.; Jin, M.; and Pfister, T. 2021. Learning and evaluating representations for deep one-class classification. In *Proceedings ICLR*.

Song, H.; Jiang, Z.; Men, A.; and Yang, B. 2017. A hybrid semi-supervised anomaly detection model for high-dimensional data. *Computational Intelligence and Neuroscience*.

Tack, J.; Mo, S.; Jeong, J.; and Shin, J. 2020. CSI: Novelty Detection via Contrastive Learning on Distributionally Shifted Instances. *NeurIPS*.

Tax, D. M.; and Duin, R. P. 2004. Support vector data description. *Machine Learning*, 54(1).

Vandermeulen, R. A.; and Scott, C. 2013. Consistency of robust kernel density estimators. In *Proceedings COLT*, 568–591.

Vyas, A.; Jammalamadaka, N.; Zhu, X.; Das, D.; Kaul, B.; and Wilke, T. L. 2018. Out-of-distribution detection using an ensemble of self-supervised leave-out classifiers. In *Proceedings ECCV*, 550–564.

Zhang, H.; Li, A.; Guo, J.; and Guo, Y. 2020. Hybrid Models for Open Set Recognition. *arXiv:2003.12506*.

## A Example of Dempster-Schafer Theory

Assume two experts have pdfs  $P_1$  and  $P_2$  defined over the power set  $2^U$  where  $U = \{a, b\}$  is the set of all possible choices. Thus, expert  $i$  has probabilities for  $P_i(\{a\}), P_i(\{b\}), P_i(\{a, b\})$  (the assumption is that probability of the null set is zero). To find  $P(\{a\})$  by combining these individual predictions, we consider all cases:  $P_1(\{a\})$  and  $P_2(\{a\})$ ,  $P_1(\{a\})$  and  $P_2(\{a, b\})$ , and  $P_1(\{a, b\})$  and  $P_2(\{a\})$ . In other words, we consider all cases when the *intersection* of the predicted sets by the two experts is  $\{a\}$ . In general, for any  $u \in 2^U, u \neq \phi$ ,

$$P(u) = \frac{1}{K} \sum_{u_1 \cap u_2 = u, u_1, u_2 \in 2^U} P_1(u_1)P_2(u_2)$$

the value  $K$  is a normalization factor and is computed as,

$$K = 1 - \sum_{u_1 \cap u_2 = \phi, u_1, u_2 \in 2^U} P_1(u_1)P_2(u_2)$$

## B Proofs for Section 3

**Lemma 3.1:** Algorithm 2 has a higher AUC value than Algorithm 1 when the same single-class anomaly detection algorithm is used in both cases.

**Proof:** Recall that the AUC value is the integral of the True Positive Rate (TPR) vs False Positive Rate (FPR) curve (each point on the curve corresponds to a different value for the detection threshold  $T$ ). For Algorithm 1 we can write the TPR and FPR as,

$$\begin{aligned} \text{TPR}_1 &= 1 - \text{False Negative Rate} \\ &= 1 - \frac{1}{K} \sum_{x_j \in \cup_{i=1}^m \mathcal{X}_i} p(x_j) \prod_{i=1}^m (1 - P_i(\{i\}|x_j)) \\ \text{FPR}_1 &= 1 - \text{True Negative Rate} \\ &= 1 - \frac{1}{K} \sum_{x_j \in \mathcal{X} \setminus \cup_{i=1}^m \mathcal{X}_i} p(x_j) \prod_{i=1}^m (1 - P_i(\{i\}|x_j)) \end{aligned}$$

Note that the difference in the two expressions is in the sets that  $x_j$  is selected from. The similar expressions for Algorithm 2 are,

$$\begin{aligned} \text{TPR}_2 &= 1 - \text{False Negative Rate} \\ &= 1 - \frac{1}{K} \sum_{x_j \in \cup_{i=1}^m \mathcal{X}_i} p(x_j) (1 - P(\text{Normal}|x_j)) \\ &= 1 - \frac{1}{K} \sum_{x_j \in \cup_{i=1}^m \mathcal{X}_i} p(x_j) \sum_{i=1}^m \frac{1}{m} (1 - P_i(\{i\}|x_j)) \\ \text{FPR}_2 &= 1 - \text{True Negative Rate} \\ &= 1 - \frac{1}{K} \sum_{x_j \in \mathcal{X} \setminus \cup_{i=1}^m \mathcal{X}_i} p(x_j) (1 - P(\text{Normal}|x_j)) \\ &= 1 - \frac{1}{K} \sum_{x_j \in \mathcal{X} \setminus \cup_{i=1}^m \mathcal{X}_i} p(x_j) \sum_{i=1}^m \frac{1}{m} (1 - P_i(\{i\}|x_j)) \end{aligned}$$

The difference in the TPR (and FPR) values of this set of expressions is that for Algorithm 1 we take a product of the form  $\prod_i (1 - P_i(\{i\}|x_j))$  whereas for Algorithm 2 this is a mean of the same probabilities. As  $m$  increases, we would expect the product term to decrease rapidly. Indeed, the values of TPR and FPR for Algorithm 1 approach 1 as  $m$  increases resulting in a purely random classifier. On the other hand, the TPR and FPR for Algorithm 2 remain relatively unchanged since they use an arithmetic mean of the probability rather than a geometric mean as in Algorithm 1. QED

**Corollary 3.1.1:** As  $m$  increases, the AUC value for Algorithm 1 decreases.

**Proof:** This is easy to see since we note that the FPR and TPR values approach 1 as  $m$  increases. QED

## C DeepMAD Architecture

We employed LeNet-type CNNs on the datasets (the same structure as DeepSVDD), where each convolutional module consists of a convolutional layer with leaky-Relu activations and  $(2 \times 2)$ -max-pooling. An encoder in DeepMAD consists of 3 such convolutional modules of filter size  $32 \times (5 \times 5)$ ,  $64 \times (5 \times 5)$ , and  $128 \times (5 \times 5)$ . Batch normalizations are applied after each convolutional module. The final layer is a dense layer of **rep\_dim** units to output the feature of **rep\_dim** dimensions (default value 128). A DeepMAD model consists of  $N$  encoders mentioned above, where  $N$  is the number of centers, and the final output is the minimum value of  $N$  encoders' outputs.

## D Best and Worst Cases for 2 in and 8 out Classes on CIFAR-10

Tables 1-5 in this section list the highest and lowest achieved AUC value for the different algorithms when 2 out of 10

classes are considered normal. The AUC values are the means over multiple runs.

DROCC (Best)	DROCC (Worst)
(0, 8) : 0.8411	(3, 9) : 0.4728
(0, 2) : 0.7252	(7, 9) : 0.4874
(2, 8) : 0.7013	(6, 9) : 0.4904
(2, 4) : 0.6878	(1, 4) : 0.4906
(0, 5) : 0.6607	(1, 5) : 0.4972
(0, 9) : 0.6596	(2, 9) : 0.5097
(0, 1) : 0.6587	(1, 3) : 0.5127
(0, 4) : 0.6567	(1, 2) : 0.5214
(0, 3) : 0.6556	(5, 9) : 0.5278
(2, 5) : 0.6501	(4, 9) : 0.5334

Table 5: Original-DROCC In-distribution classes (2 out of 10) of CIFAR-10 with best and worst 10 AUC value.

DROCC(2) (Best)	DROCC(2) (Worst)
(0, 8) : 0.8255	(7, 9) : 0.4216
(0, 2) : 0.7283	(3, 9) : 0.4584
(2, 8) : 0.6912	(4, 9) : 0.4596
(2, 5) : 0.6700	(1, 7) : 0.4686
(0, 3) : 0.6583	(6, 9) : 0.4846
(2, 4) : 0.6553	(1, 6) : 0.4887
(0, 4) : 0.6545	(5, 9) : 0.4985
(8, 9) : 0.6539	(3, 6) : 0.4991
(0, 5) : 0.6505	(5, 6) : 0.5008
(0, 1) : 0.6500	(1, 5) : 0.5011

Table 6: DROCC(2) In-distribution classes (2 out of 10) of CIFAR-10 with best and worst 10 AUC value.

DeepSVDD (Best)	DeepSVDD (Worst)
(4, 6) : 0.7554	(1, 7) : 0.4112
(2, 4) : 0.7150	(1, 5) : 0.4210
(2, 6) : 0.7103	(5, 9) : 0.4262
(4, 8) : 0.6830	(1, 3) : 0.4362
(0, 6) : 0.6624	(7, 9) : 0.4594
(0, 4) : 0.6597	(3, 9) : 0.4600
(4, 5) : 0.6525	(1, 9) : 0.4661
(6, 8) : 0.6482	(5, 7) : 0.4730
(3, 4) : 0.6408	(0, 1) : 0.4743
(3, 6) : 0.6344	(0, 9) : 0.4825

Table 7: DeepSVDD(2) In-distribution classes (2 out of 10) of CIFAR-10 with best and worst 10 AUC value.

## E Best and Worst Cases for 2 in 18 out Classes on CIFAR-100

For CIFAR-100 we have 190 possible combinations of 2 normal classes and 18 anomalous classes. We ran the three algorithms – DROCC, DeepSVDD, and DeepMAD on all these cases and the tables summarize the best and worst combinations based on AUC values. This information is presented in Tables 6-8.

DeepSVDD(2) (Best)	DeepSVDD(2) (Worst)
(4, 6) : 0.7516	(1, 5) : 0.4147
(2, 4) : 0.7206	(1, 7) : 0.4206
(2, 6) : 0.7136	(5, 9) : 0.4317
(4, 8) : 0.6844	(1, 3) : 0.4357
(0, 4) : 0.6588	(7, 9) : 0.4605
(6, 8) : 0.6526	(3, 9) : 0.4608
(0, 6) : 0.6443	(1, 9) : 0.4723
(3, 6) : 0.6388	(0, 9) : 0.4758
(0, 2) : 0.6367	(5, 7) : 0.4803
(4, 5) : 0.6352	(3, 7) : 0.4863

Table 8: DeepSVDD In-distribution classes (2 out of 10) of CIFAR-10 with best and worst 10 AUC value.

DeepMAD (Best)	DeepMAD (Worst)
(6, 8) : 0.7654	(3, 5) : 0.5277
(0, 6) : 0.7627	(3, 9) : 0.5791
(6, 7) : 0.7529	(1, 3) : 0.5834
(0, 9) : 0.7270	(0, 2) : 0.5863
(4, 8) : 0.7245	(3, 6) : 0.5941
(6, 9) : 0.7200	(7, 9) : 0.5983
(1, 8) : 0.7188	(3, 8) : 0.6023
(0, 1) : 0.7174	(2, 3) : 0.6047
(5, 6) : 0.7142	(2, 5) : 0.6105
(4, 9) : 0.7141	(1, 9) : 0.6194

Table 9: DeepMAD In-distribution classes (2 out of 10) of CIFAR-10 with best and worst 10 AUC value.

## F Best and Worst Cases for 5 in 5 out Classes

For the case when 5 classes are normal and 5 are anomalous (for CIFAR-10) we have a total of 252 combinations. We report on the top ten and worst ten for each of the five algorithms in Tables 9-13.

## G Hyper-Parameters

Table 18-20 shows the hyper-parameters for all the networks we used for testing in the paper.

## H Tuning DeepMAD

We conducted experiments where we added a 64 or a 32 dimensional layer after the last 128 dimensional layer of the encoder. We observe that for the CIFAR-10 2 in/8 out case, DeepMAD performs equally well for all three instances as shown in Figure 8.

DROCC(2) (Best)	DROCC(2) (Worst)
(1, 10) : 0.7341	(2, 18) : 0.3548
(9, 10) : 0.7323	(2, 19) : 0.3995
(0, 10) : 0.7279	(2, 6) : 0.4259
(6, 10) : 0.7200	(14, 18) : 0.4354
(10, 17) : 0.7128	(0, 2) : 0.4379
(3, 10) : 0.7080	(8, 19) : 0.4433
(10, 16) : 0.6897	(2, 7) : 0.4485
(6, 9) : 0.6824	(2, 14) : 0.4488
(10, 13) : 0.6736	(8, 18) : 0.4509
(10, 19) : 0.6722	(18, 19) : 0.4622

Table 10: DROCC(2) In-distribution (super) classes (2 out of 20) of CIFAR-100 with best and worst 10 AUC value.

DROCC(5) (Best)	DROCC(5) (Worst)
(0, 2, 4, 5, 8) : 0.7023	(1, 4, 6, 7, 9) : 0.3806
(0, 2, 4, 7, 8) : 0.6615	(1, 5, 6, 7, 9) : 0.3813
(0, 2, 4, 6, 8) : 0.6401	(1, 3, 6, 7, 9) : 0.3832
(2, 3, 4, 5, 7) : 0.6277	(1, 4, 5, 6, 9) : 0.4041
(0, 1, 2, 4, 8) : 0.6215	(1, 3, 6, 8, 9) : 0.4185
(2, 3, 4, 5, 6) : 0.6162	(1, 6, 7, 8, 9) : 0.4219
(0, 2, 7, 8, 9) : 0.6154	(1, 2, 6, 7, 9) : 0.4257
(0, 2, 4, 8, 9) : 0.6012	(0, 1, 6, 7, 9) : 0.4449
(0, 2, 6, 7, 8) : 0.5901	(5, 6, 7, 8, 9) : 0.4485
(0, 2, 6, 8, 9) : 0.5540	(1, 4, 5, 6, 7) : 0.4525

Table 14: DROCC(2) In-distribution classes (5 out of 10) of CIFAR-10 with best and worst 10 AUC value.

DeepSVDD(2) (Best)	DeepSVDD(2) (Worst)
(10, 17) : 0.7185	(14, 18) : 0.4196
(9, 10) : 0.7077	(2, 14) : 0.4226
(8, 10) : 0.6962	(1, 18) : 0.4255
(10, 16) : 0.6941	(5, 14) : 0.4258
(10, 12) : 0.6864	(5, 18) : 0.4318
(10, 11) : 0.6740	(6, 14) : 0.4361
(10, 13) : 0.6731	(5, 19) : 0.4372
(0, 10) : 0.6647	(14, 19) : 0.4378
(10, 15) : 0.6478	(6, 18) : 0.4426
(0, 17) : 0.6420	(6, 19) : 0.4435

Table 11: DeepSVDD(2) In-distribution (super) classes (2 out of 20) of CIFAR-100 with best and worst 10 AUC value.

DeepSVDD (Best)	DeepSVDD (Worst)
(0, 2, 3, 4, 6) : 0.7105	(1, 3, 5, 7, 9) : 0.3382
(2, 3, 4, 5, 6) : 0.7047	(0, 1, 5, 7, 9) : 0.3484
(0, 2, 4, 6, 8) : 0.6974	(0, 1, 3, 5, 9) : 0.3556
(0, 2, 4, 6, 7) : 0.6970	(1, 5, 7, 8, 9) : 0.3654
(0, 2, 4, 5, 6) : 0.6953	(1, 3, 5, 8, 9) : 0.3674
(2, 3, 4, 6, 8) : 0.6886	(0, 1, 3, 7, 9) : 0.3690
(2, 4, 5, 6, 8) : 0.6801	(1, 3, 7, 8, 9) : 0.3880
(2, 4, 5, 6, 7) : 0.6765	(0, 1, 5, 7, 8) : 0.3881
(2, 4, 6, 7, 8) : 0.6762	(0, 1, 3, 5, 7) : 0.3882
(2, 3, 4, 6, 7) : 0.6714	(0, 3, 5, 7, 9) : 0.3890

Table 15: DeepSVDD In-distribution classes (5 out of 10) of CIFAR-10 with best and worst 10 AUC value.

DeepMAD (Best)	DeepMAD (Worst)
(2, 10) : 0.8213	(13, 15) : 0.5384
(2, 17) : 0.8044	(8, 12) : 0.5484
(10, 17) : 0.7967	(7, 13) : 0.5496
(6, 17) : 0.7958	(15, 16) : 0.5556
(3, 17) : 0.7796	(13, 16) : 0.5561
(2, 9) : 0.7750	(8, 11) : 0.5575
(4, 10) : 0.7745	(12, 16) : 0.5606
(14, 17) : 0.7690	(4, 13) : 0.5647
(1, 17) : 0.7681	(12, 15) : 0.5647
(10, 14) : 0.7663	(2, 13) : 0.5650

Table 12: DeepMAD In-distribution (super) classes (2 out of 20) of CIFAR-100 with best and worst 10 AUC value.

DeepSVDD(5) (Best)	DeepSVDD(5) (Worst)
(0, 2, 3, 4, 6) : 0.6909	(1, 3, 5, 8, 9) : 0.3482
(0, 2, 4, 6, 8) : 0.6837	(1, 3, 7, 8, 9) : 0.3711
(2, 3, 4, 5, 6) : 0.6814	(0, 1, 5, 7, 9) : 0.3715
(0, 2, 4, 5, 6) : 0.6799	(1, 3, 5, 7, 9) : 0.3733
(0, 2, 4, 6, 7) : 0.6787	(0, 1, 3, 5, 9) : 0.3886
(2, 3, 4, 6, 7) : 0.6659	(1, 2, 5, 7, 9) : 0.3934
(2, 3, 4, 6, 8) : 0.6566	(1, 3, 5, 7, 8) : 0.3947
(2, 4, 5, 6, 8) : 0.6465	(1, 5, 7, 8, 9) : 0.3979
(0, 1, 2, 4, 6) : 0.6460	(0, 1, 3, 7, 9) : 0.4032
(2, 4, 5, 6, 7) : 0.6452	(1, 2, 3, 5, 9) : 0.4056

Table 16: DeepSVDD(2) In-distribution classes (5 out of 10) of CIFAR-10 with best and worst 10 AUC value.

DROCC (Best)	DROCC (Worst)
(0, 2, 3, 5, 8) : 0.7219	(0, 1, 5, 6, 9) : 0.4316
(0, 2, 4, 5, 8) : 0.7157	(0, 1, 3, 6, 9) : 0.4519
(0, 2, 3, 4, 8) : 0.7028	(0, 1, 2, 6, 9) : 0.4556
(0, 2, 4, 7, 8) : 0.6863	(0, 1, 4, 6, 7) : 0.4601
(0, 2, 5, 8, 9) : 0.6743	(0, 1, 5, 6, 7) : 0.4686
(0, 1, 2, 5, 8) : 0.6716	(0, 1, 4, 6, 9) : 0.4687
(0, 2, 3, 7, 8) : 0.6696	(0, 4, 5, 6, 9) : 0.4704
(0, 2, 3, 4, 5) : 0.6634	(0, 5, 6, 7, 9) : 0.4885
(0, 2, 5, 7, 8) : 0.6620	(0, 3, 4, 6, 9) : 0.4936
(0, 3, 4, 5, 8) : 0.6606	(0, 1, 3, 6, 7) : 0.5041

Table 13: DROCC In-distribution classes (5 out of 10) of CIFAR-10 with best and worst 10 AUC value.

DeepMAD (Best)	DeepMAD (Worst)
(0, 5, 6, 7, 8) : 0.7738	(0, 1, 3, 8, 9) : 0.4929
(0, 2, 6, 7, 8) : 0.7660	(3, 4, 5, 7, 9) : 0.5408
(0, 4, 6, 7, 8) : 0.7620	(0, 1, 2, 8, 9) : 0.5463
(1, 2, 6, 7, 8) : 0.7566	(2, 3, 5, 7, 9) : 0.5518
(2, 6, 7, 8, 9) : 0.7438	(0, 1, 5, 8, 9) : 0.5553
(0, 3, 6, 7, 8) : 0.7436	(2, 3, 5, 6, 9) : 0.5642
(1, 4, 6, 7, 8) : 0.7432	(3, 4, 5, 6, 9) : 0.5655
(0, 4, 5, 6, 8) : 0.7383	(0, 1, 4, 8, 9) : 0.5726
(0, 2, 4, 6, 8) : 0.7221	(3, 5, 6, 7, 9) : 0.5860
(2, 4, 6, 8, 9) : 0.7059	(0, 1, 7, 8, 9) : 0.6156

Table 17: DeepMAD-In-distribution classes (5 out of 10) of CIFAR-10 with best10 and worst10 AUC value.

Radius	$\mu$	Optimizer	Learning Rate	Adversarial Ascent Step Size
8	1	Adam	0.001	0.001

Table 18: HyperParameters: DROCC

$\eta$	$\epsilon$	Optimizer	Learning Rate	Weight Decay	rep_dim
1.0	0.01	Adam	0.0001	$1e^{-6}$	128

Table 19: HyperParameters: DeepSVDD

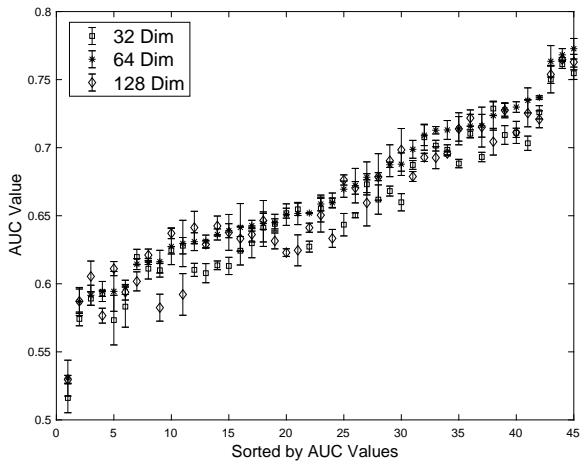


Figure 8: DeepMAD with different feature vector dimensions.

$\eta$	$\delta$	Optimizer	Learning Rate	Weight Decay	rep_dim
1.0	8.0	Adam	0.0001	$1e^{-6}$	128
1.0	8.2	Adam	0.0001	$1e^{-6}$	128
1.0	8.5	Adam	0.0001	$1e^{-6}$	128
1.0	8.2	Adam	0.0001	$1e^{-6}$	64
1.0	8.2	Adam	0.0001	$1e^{-6}$	32

Table 20: HyperParameters: DeepMAD

DROCC										DeepSVDD									
0	1	2	3	4	5	6	7	8	9	0	1	2	3	4	5	6	7	8	9
KS((0,8),-), AUC = 0.84										KS((4,6),-), AUC = 0.75									
0	63	57	61	61	61	64	63	0	63	37	45	9	30	0	24	0	29	36	49
KS((5,9),-), AUC = 0.5										KS((1,5),-), AUC = 0.41									
45	12	36	50	51	14	52	31	38	14	28	0	18	13	18	0	34	15	31	14

Table 21:  $h$  value for the KS test for DROCC and DeepSVDD.

		0	1	2	3	4	5	6	7	8	9
In classes (0,1), AUC=0.7174	KS(0, -)	<b>0</b>	<b>100</b>	44	127	124	128	126	128	60	125
	KS(1,-)	<b>100</b>	<b>0</b>	101	123	118	123	123	121	107	124
In classes (3,5), AUC=0.5277	KS(3, -)	16	1	4	<b>0</b>	16	<b>96</b>	2	73	81	99
	KS(5,-)	96	94	77	<b>96</b>	87	<b>0</b>	97	29	105	106

Table 22:  $h$  value for the KS test for DeepMAD.